A Hamilton-Jacobi-Bellman approach to high angular resolution diffusion tractography

Eric Pichon[1], Carl-Fredrik Westin[2] and Allen Tannenbaum[1]

[1] Georgia Institute of Technology, Atlanta GA 30332, USA
{`eric, tannenba`}`@ece.gatech.edu`,
[2] Harvard Medical School, Boston, MA 02115, USA
`westin@bwh.harvard.edu`

Abstract. This paper describes a new framework for white matter tractography in high angular resolution diffusion data. A direction-dependent local cost is defined based on the diffusion data for every direction on the unit sphere. Minimum cost curves are determined by solving the Hamilton-Jacobi-Bellman using an efficient algorithm. Classical costs based on the diffusion tensor field can be seen as a special case. While the minimum cost (or equivalently the travel time of a particle moving along the curve) and the anisotropic front propagation frameworks are related, front speed is related to particle speed through a Legendre transformation which can severely impact anisotropy information for front propagation techniques. Implementation details and results on high angular diffusion data show that this method can successfully take advantage of the increased angular resolution in high b-value diffusion weighted data despite lower signal to noise ratio.

1 Introduction

The development of Diffusion Tensor MRI has raised hopes in the neuroscience community for in vivo methods to track fiber paths in white matter. Diffusion Tensor Magnetic Resonance Imaging (DT-MRI) measures the self-diffusion of water in biological tissue [1]. The utility of this method stems from the fact that tissue structure locally affects the Brownian motion of water molecules and will be reflected in the DT-MRI diffusion measurements. In classical theory, diffusion follows a Gaussian process which can be described locally by a second order tensor.

A simple and effective method for tracking nerve fibers using DT-MRI is to follow the direction of maximum diffusion at each voxel [2,3,4,5]. Although this method is widely spread and used in various ways the fiber trajectory is based solely on local information which makes it very sensitive to noise. Moreover the major direction of diffusion can become ill-defined for example at fiber crossings.

It has been proposed to shift from the Lagrangian, particle[3] based streamline approach described above to a Eulerian front propagation approach that can use

---

[3] In this work, "particle" refers to the position of a fictitious evolving point

full tensor information and is more robust to noise [6,7]. This can be set in a Riemannian framework [8,9].

The Gaussian assumption of diffusion tensor imaging does not hold for example if several fibers with different directions co-exist within the same voxel. Extensions to the tensor model have been proposed [10]. High angular resolution diffusion modalities such as Q-Ball imaging [11] acquire diffusion information in potentially hundreds of directions thus measuring direction information in a non-parametric way. Hagmann *et al.* [12] extend the streamline technique to multi-valued vector fields and Campbell [13] proposes a front evolution approach based on high angular resolution data.

In this work tractography is set in a continuous minimum cost framework. This is different from [12,13] who do not propose variational (cost minimizing) techniques. Local costs are defined for every direction on the unit sphere based on high angular resolution diffusion imagery. Equivalently this can be considered a minimum arrival time framework in which the speed of fictitious particles would be the inverse of the cost. We show that while the minimum arrival time and anisotropic front propagation frameworks are deeply related, front speed is related to particle speed through a Legendre transformation [14] which can severely impact anisotropy information for front propagation techniques (Section 2). Implementation details for our technique are discussed (Section 3) along with considerations on the definition of the cost and the use of prior information (Section 4). Finally, the technique is illustrated on high angular resolution diffusion imagery (Section 5). Due to space constraints, full details will be published in [15].

2 Theory

2.1 Direction-Dependent Local Costs

Minimum cost approaches have been used extensively in image segmentation. In active contour models, an initial curve $\boldsymbol{\Gamma}(t = 0)$ is continually deformed using calculus of variations in a way that optimally minimizes a global cost $C(\boldsymbol{\Gamma}(t))$. This global cost is obtained by integrating along the curve a local cost, $\Psi : \mathbb{R}^n \to \mathbb{R}^+$ based on image information. The Live-Wire algorithm [16] determines all the optimal curves between a seed region and any pixel of the image using dynamic programming.

We propose to extend these two techniques to directional data by considering direction-dependent local costs of the form[4] $\Psi : \mathbb{R}^n \times \mathbb{S}^{n-1} \to \mathbb{R}^+$. The global cost of a given curve $\boldsymbol{\Gamma}$, is then defined to be

$$C(\boldsymbol{\Gamma}) \triangleq \int_{\boldsymbol{\Gamma}} \Psi(\boldsymbol{\Gamma}, \hat{\boldsymbol{\Gamma}}_s) \, \mathrm{d}s, \tag{1}$$

which depends locally not only on the position of the curve but also on the direction of its unit tangent $\hat{\boldsymbol{\Gamma}}_s$.

---

[4] A position $\boldsymbol{p}$ in n-dimensional space $\mathbb{R}^n$ is written in bold, and a hat denotes a direction $\hat{\boldsymbol{d}}$ of the unit sphere $\mathbb{S}^{n-1}$.

2.2 Calculus of Variations

The first variation of the functional (1) can be computed which leads to the optimal minimizing deformation

$$\frac{\partial \boldsymbol{\Gamma}}{\partial t} = -P_{\hat{\boldsymbol{\Gamma}}_s^{\perp}}(\ \nabla_{\boldsymbol{\Gamma}}\Psi - \frac{\partial}{\partial s}\nabla_{\hat{\boldsymbol{\Gamma}}_s}\Psi \ ) + \Psi\boldsymbol{\Gamma}_{ss}, \tag{2}$$

where $P_{\hat{\boldsymbol{\Gamma}}_s^{\perp}}$ is the projection onto the plane normal to $\hat{\boldsymbol{\Gamma}}_s$ and any user-defined direction-dependent cost $\Psi(\boldsymbol{\Gamma}, \hat{\boldsymbol{\Gamma}}_s)$ can be used. This result extends minimizing flows for functional of the form $C(\boldsymbol{\Gamma}) = \int_{\boldsymbol{\Gamma}} \boldsymbol{v}.\hat{\boldsymbol{\Gamma}}_s \ \mathrm{d}s$, proposed independently for tractography [13,17].

2.3 Dynamic Programming

This technique is based on defining a value function $C^*(\boldsymbol{p})$ that represents, for any point $\boldsymbol{p}$ in the domain, the minimum cost over all curves between $\boldsymbol{p}$ and the region S. From any $\boldsymbol{p}$, the optimal curve back to S is obtained by descent on C^*. It can be shown that the value function C^* satisfies the Hamilton-Jacobi-Bellman equation

$$\max_{\hat{\boldsymbol{d}} \in \mathbb{S}^{n-1}} \{ \ \nabla C^*(\boldsymbol{p}).\hat{\boldsymbol{d}} - \Psi(\boldsymbol{p}, \hat{\boldsymbol{d}}) \ \} = 0. \tag{3}$$

The cost Ψ can be interpreted as the inverse of the speed of a particle traveling along the curve. $C^*(\boldsymbol{p})$ is then the minimum arrival time at $\boldsymbol{p}$. Alternatively, an infinite number of particle departing from S at the same time would propagate as a front geometrically evolving in the direction of its normal with a speed F. The corresponding equation is $\|\nabla C^*(\boldsymbol{p})\|F(\boldsymbol{p}, \nabla C^*(\boldsymbol{p})/\|\nabla C^*(\boldsymbol{p})\|) = 1$. The two speeds F and $1/\Psi$ are not identical because particles are not restricted to moving along the normal of the evolving front. Front speed and cost (or its inverse, particle speed) are related through the Legendre transformations [14]

$$F(\boldsymbol{p}, \hat{\boldsymbol{n}}) = 1/ \min_{\hat{\boldsymbol{d}}.\hat{\boldsymbol{n}}>0} \{ \ \frac{\Psi(\boldsymbol{p}, \hat{\boldsymbol{n}})}{\hat{\boldsymbol{d}}.\hat{\boldsymbol{n}}} \ \} \text{ and } \Psi(\boldsymbol{p}, \hat{\boldsymbol{d}}) = \max_{\hat{\boldsymbol{d}}.\hat{\boldsymbol{n}}>0} \{ \ (\hat{\boldsymbol{d}}.\hat{\boldsymbol{n}})/F(\boldsymbol{p}, \hat{\boldsymbol{n}}) \ \}. \tag{4}$$

Anisotropic front propagation techniques are not set in a Hamilton-Jacobi-Bellman framework. Consequently it is the front speed F which is defined from the diffusion data. Curves will then be determined that are optimal for C, which can only be interpreted as a cost (or an arrival time) in terms of Ψ. The *max* operator present in the definition of Ψ from F will tend to filter out the highest values of the front speed F that correspond to the preferred spatial directions (and therefore potential fibers) while preserving the slowest directions. Simulations and further analysis show that this distortion affects particularly speed functions with very localized direction information such as those encountered in high angular resolution diffusion imagery and can even result in loss of information. This problem can be avoided by setting directly the problem in a minimum cost framework (as proposed) or taking into account the Legendre transformation (4) when defining F.

Given the boundary condition $C^* = 0$ on some seed region S the Hamilton-Jacobi-Bellman equation (3) can be solved for the value function C^* as well as the characteristic direction $\hat{\boldsymbol{d}}^*$. Then, from any point $\boldsymbol{p}$, an optimal curve $\boldsymbol{\Gamma}^*(\boldsymbol{p})$ can be determined back to S by following the characteristics $\hat{\boldsymbol{d}}^*$. By construction, $C(\boldsymbol{\Gamma}^*(\boldsymbol{p}))$ equals the optimal cost $C^*(\boldsymbol{p})$. For these C-optimal curves, the value of another global cost, K, corresponding to a different local cost Φ can be computed by solving the transport equation

$$\nabla K(\boldsymbol{p}).\hat{\boldsymbol{d}}^*(\boldsymbol{p}) = \Phi(\boldsymbol{p}, \hat{\boldsymbol{d}}^*(\boldsymbol{p})) \tag{5}$$

with boundary condition $K = 0$ on the seed region S. In particular the length $L(\Gamma^*(\boldsymbol{p})) = \int_{\boldsymbol{\Gamma}^*(\boldsymbol{p})} 1 \, \mathrm{d}s$ of these optimal curves corresponds to $\Phi = 1$. The cost per unit length K/L can be used to define a validity index and rank curves that are optimal for one criterion using another criterion as in [6,7].

3 Implementation

The HBJ equation (3) can be solved using a fast sweeping numerical scheme proposed by Kao *et al.* [18], similar to the one used in [7]. The algorithm

---

Algorithm 1 Sweeping algorithm to solve the Hamilton-Jacobi-Bellman equation (3), see [18]

Require: seed region S, direction-dependent local cost Ψ
1: Initialize $C^*(\cdot) \leftarrow +\infty$, except at starting points $s \in S$ where $C^*(s) \leftarrow 0$
2: **repeat**
3:     **sweep** through all voxels $\boldsymbol{p}$, in all possible grid directions
4:        $\hat{\boldsymbol{d}}' \leftarrow \arg\min_{d \in \mathbb{S}^{n-1}} f_{C^*,\Psi}(\boldsymbol{p}, \hat{\boldsymbol{d}})$
5:        **if** $f_{C^*,\Psi}(\boldsymbol{p}, \hat{\boldsymbol{d}}') < C^*(\boldsymbol{p})$ **then** $C^*(\boldsymbol{p}) \leftarrow f_{C^*,\Psi}(\boldsymbol{p}, \hat{\boldsymbol{d}}')$ and $\hat{\boldsymbol{d}}^*(\boldsymbol{p}) \leftarrow \hat{\boldsymbol{d}}'$ **end if**
6:     **end sweep**
7: **until** convergence of C^*
8: **return** value function C^*, characteristics $\hat{\boldsymbol{d}}^*$

---

sweeps through all points $\boldsymbol{p}$ in search of the least expensive direction. The cumulated cost to reach $\boldsymbol{p}$ from direction $\hat{\boldsymbol{d}}$ is $f_{C^*,\Psi}(\boldsymbol{p}, \hat{\boldsymbol{d}}) \triangleq (\sum_{k=1}^{n} \alpha_k C^*(\boldsymbol{p} + \boldsymbol{\delta}_k) + \Psi(\boldsymbol{p}, \hat{\boldsymbol{d}}))/(\sum_{k=1}^{n} \alpha_k)$, where the n neighbors[5] $\boldsymbol{p} + \boldsymbol{\delta}_1, \dots, \boldsymbol{p} + \boldsymbol{\delta}_n$ of $\boldsymbol{p}$ in direction $\hat{\boldsymbol{d}}$ are interpolated using the components of the vector $\boldsymbol{\alpha} \triangleq [\boldsymbol{\delta}_1 \mid \dots \mid \boldsymbol{\delta}_n]^{-1}\hat{\boldsymbol{d}}$. For example, if $\hat{\boldsymbol{d}} = \boldsymbol{\delta}_k/\|\boldsymbol{\delta}_k\|$ (i.e., $\hat{\boldsymbol{d}}$ points directly at one of the neighboring voxels) then $f = C^*(\boldsymbol{p} + \boldsymbol{\delta}_k) + \Psi(\boldsymbol{p}, \hat{\boldsymbol{d}})\|\boldsymbol{\delta}_k\|$. While this is reminiscent of Dijkstra's algorithm, the search for the optimal direction is not restricted to

---

[5] in 3D, this is $n = 3$ neighbors among 26.

discrete grid directions. In our implementation the minimization is performed over 100 directions sampled uniformly on the sphere and the coefficients $\boldsymbol{\alpha}(\hat{\boldsymbol{d}})$ are pre-computed.

Once the vector field $\hat{\boldsymbol{d}}^*$ is known, a slightly modified[6] version of Algorithm 1 is used to solve transport equations.

4 Application to High Angular Diffusion MRI Tractography

4.1 Constructing the Direction-Dependent Cost

Most front propagation techniques for diffusion tensor tractography use some ad hoc function f of the quadratic form $\hat{\boldsymbol{d}}^t D \hat{\boldsymbol{d}}$. If the Gaussian assumption holds, the diffusion weighted images follow $S(\boldsymbol{p}, \hat{\boldsymbol{d}}) \simeq S(\boldsymbol{p}, \boldsymbol{0}) \exp(-b\,\hat{\boldsymbol{d}}^t D(\boldsymbol{p}) \hat{\boldsymbol{d}})$. Tensor based techniques can formally be extended to high angular resolution diffusion datasets by setting

$$\Psi(\boldsymbol{p}, \hat{\boldsymbol{d}}) \triangleq f(-\frac{1}{b}\log(\frac{S(\hat{\boldsymbol{d}})}{S(\boldsymbol{0})})) \tag{6}$$

Notice that Q-Ball datasets [11] and direction-dependent local costs Ψ are both defined on the same space $\mathbb{R}^3 \times \mathbb{S}^2$.

However, due to the low signal to noise ratio of these datasets, it is desirable to consider more than one value at a time. The anisotropic cost can be defined by some decreasing function f' of the Funk-Radon transform[7] of the attenuation $S(\boldsymbol{p}, \cdot)/S(\boldsymbol{p}, \boldsymbol{0})$.

$$\Psi'(\boldsymbol{p}, \hat{\boldsymbol{d}}) \triangleq f'(\int_{\hat{\boldsymbol{v}} \perp \hat{\boldsymbol{d}}} \frac{S(\hat{\boldsymbol{v}})}{S(\boldsymbol{0})}\ \mathrm{d}\hat{\boldsymbol{v}}) \tag{7}$$

The cost $\Psi'(\boldsymbol{p}, \hat{\boldsymbol{d}})$ will therefore be small if and only if there is limited diffusion loss over the corresponding equator, i.e., if diffusion does not occur normal to $\hat{\boldsymbol{d}}$.

4.2 Using Prior Knowledge

Mumford [19] showed that variational techniques, such as the one proposed here, can be set in an elegant and principled Bayesian framework by considering the cost $\Psi = \Psi_{\text{data}} + \Psi_{\text{prior}}$. The extreme simplicity of this construction constitutes another advantage over non-variational front propagation approaches. Here, Ψ_{data} would be as described above and Ψ_{prior} could be obtained from an atlas of neural tracts.

The problems of generating such an atlas and registering it to the dataset at hand are well beyond the scope of this paper. Note however that masking off (with infinite cost values) the non white matter regions of the brain is a trivial and widely employed use of prior knowledge.

---

[6] no minimization needs to be performed

[7] Interestingly, the FRT is also central to the Q-Ball technique [11].

5 Results

Here we show results obtained by applying the methodology described in the above sections to diffusion weighted data sets acquired using a single-shot diffusion-weighted EPI sequence, with 31 different gradient directions with b-values of 500, 1000, and 1500 s/mm2, on a 1.5 Tesla GE Echospeed system. The data was acquired with different b-values to enable comparisons of the results. Traditional eigenvector based tractography is normally carried out in data with b-values in the range of 700-1000 s/mm^2. Higher b-values give data with higher angular contrast but at the expense of more noise.

Cost per unit length, which can be interpreted as a validity index for the putative tracts was determined for all b-values Fig. 1. All curves are optimal given

(a) $b = 500$ (b) $b = 1000$ (c) $b = 1500$
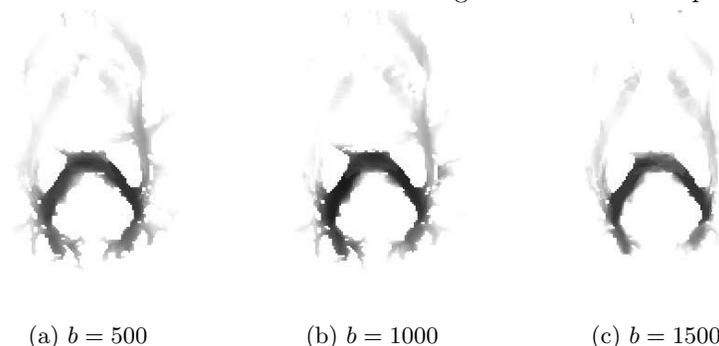
Fig. 1. Cost per unit length of end points of optimal curves for different b-values is a validity index (see text). Best results are achieved for the highest b-value.

their starting point. The cost per unit length is a measure of how good they are compared to each other. The best contrast (corresponding to the most coherent set of "super-optimal" tracts for a given seed point posterior of the corpus callosum) was obtained at the highest b-value available. This could indicate that the algorithm was was able to take advantage of the higher angular contrast in spite of the lower SNR.

Tract results for several user defined seed points are presented on Fig. 2.

Finally the proposed technique was compared to a streamline technique for the needs of which the tensor field was computed (Fig. 3). While validation is a very challenging task due to the unavailability of ground truth, it can be noted that both algorithm give similar results even though their inputs are different. The tracts of the proposed technique tend to be more coherent as any noise in the data might set the streamline off course whereas the proposed technique is more global.

6 Conclusion

A novel technique has been proposed for fiber tractography from high angular resolution diffusion imagery. In difference to [12,13] this is based on a princi-

(a)   (b)
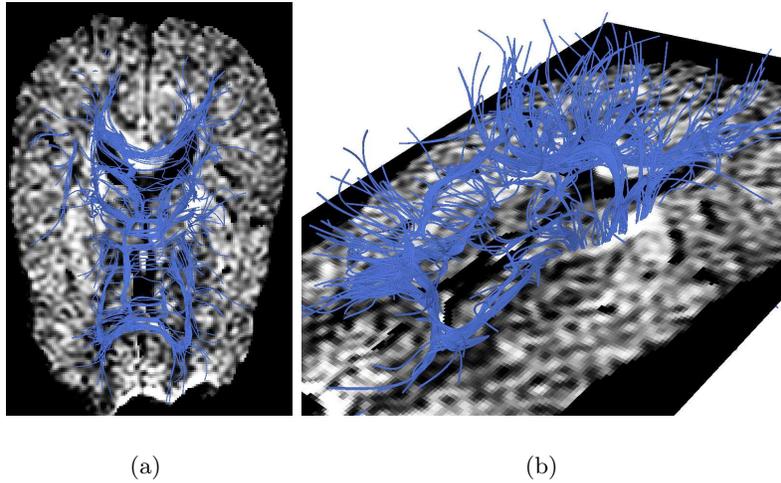
Fig. 2. Fiber tracking from high angular resolution dataset (b=1500 s/mm^2).
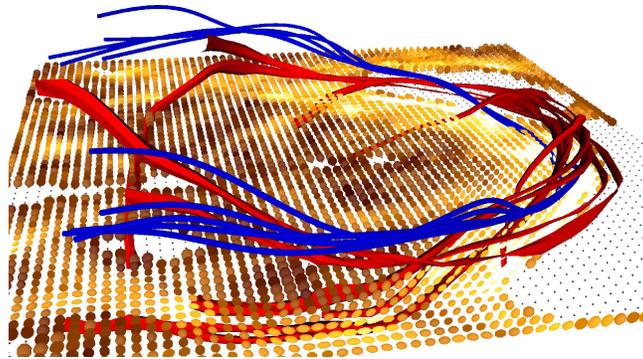
Fig. 3. Proposed technique on high angular resolution data (blue) compared with streamline technique on tensor field (red) (b=1500 s/mm^2).

pled minimum cost (or arrival time) approach. By setting front propagation techniques in a variational light the proposed technique gives some insights on the interpretation of front speed versus particle speed. Preliminary results show that the technique performs better for high b-values when directional resolution is higher. Further research topics include detailed validation as well as the use of prior information.

Acknowledgments

References

1. Basser, P., Mattiello, J., LeBihan, D.: MR diffusion tensor spectroscopy and imaging. Biophys. J. **66** (1994) 259–267
2. Mori, S., Crain, B., Chacko, V., van Zijl, P.: Three-dimensional tracking of axonal projections in the brain by magnetic resonance imaging. Ann Neurol. **45** (1999) 265–269
3. Conturo, T., Lori, N., Cull, T., Akbudak, E., Snyder, A., Shimony, J., McKinstry, R., Burton, H., Raichle, M.: Tracking neuronal fiber pathways in the living human brain. In: Proc. Natl. Acad. Sci. USA. (1999) 10422–10427
4. Westin, C.F., Maier, S.E., Khidhir, B., Everett, P., Jolesz, F.A., Kikinis, R.: Image processing for diffusion tensor magnetic resonance imaging. In: MICCAI. (1999) 441–452
5. Basser, P., Pajevic, S., Pierpaoli, C., Duda, J., Aldroubi, A.: In vivo fiber tractography using DT-MRI data. Magnetic Resonance in Medicine **44** (2000) 625–632
6. Parker, G., Wheeler-Kingshott, C., Barker, G.: Estimating distributed anatomical connectivity using fast marching methods and diffusion tensor imaging. IEEE Transactions on Medical Imaging **21** (2002) 505–512
7. Jackowski, M., Kao, C.Y., Qiu, M., Constable, R.T., Staib, L.: Estimation of anatomical connectivity by anisotropic front propagation and diffusion tensor imaging. In: MICCAI. (2004) 663–671
8. O'Donnell, L., Haker, S., Westin, C.F.: New approaches to estimation of white matter connectivity in diffusion tensor MRI: Elliptic PDEs and geodesics in a tensor-warped space. In: MICCAI. (2002)
9. Lenglet, C., Deriche, R., Faugeras, O.: Inferring white matter geometry from diffusion tensor MRI: Application to connectivity mapping. In: ECCV. (2004)
10. Liu, C., Bammer, R., Acar, B., Moseley, M.: Characterizing non-Gaussian diffusion by using generalized diffusion tensors. Magnetic Resonance in Medicine **51** (2004) 924–937
11. Tuch, D.: Q-ball imaging. Magn Reson Med. **52** (2004) 1358–1372
12. Hagmann, P., Reese, T.G., Tseng, W.Y.I., Meuli, R., Thiran, J.P., Wedeen, V.J.: Diffusion spectrum imaging tractography in complex cerebral white matter: an investigation of the centrum semiovale. In: ISMRM. (2004)
13. Campbell, J.S.: Diffusion Imaging of White Matter Fibre Tracts. PhD thesis, McGill University (2004)
14. Strang, G.: Introduction to Applied Mathematics. Wellesley-Cambridge Press (1986)
15. Pichon, E. PhD thesis, Department of Electrical and Computer Engineering, Georgia Institute of Technology (2005)
16. Mortensen, E., Morse, B., Barrett, W., Udupa, J.: Adaptive boundary detection using live-wire two-dimensional dynamic programming. In: IEEE Proceedings of Computers in Cardiology. (1992) 635–638
17. Pichon, E., Sapiro, G., Tannenbaum, A.: Segmentation of Diffusion Tensor Imagery. Number 286 in LNCIS. In: Directions in Mathematical Systems Theory and Optimization. (2003) 239–247
18. Kao, C., Osher, S., Tsai, Y.: Fast sweeping methods for static Hamilton-Jacobi equations. Technical Report 03-75, UCLA CAM (2003)
19. Mumford, D.: The Bayesian Rationale for Energy Functionals. In: Geometry-driven Diffusion in Computer Vision. Kluwer Academic Publisher (1994) 141–153